J Solid State Electrochem (2012) 16:3105–3114
DOI 10.1007/s10008-012-1733-4

ORIGINAL PAPER

Enhanced zinc ion transport in gel polymer electrolyte: effect of nano-sized ZnO dispersion

Sellam · S. A. Hashmi

Received: 21 July 2011 / Revised: 21 November 2011 / Accepted: 19 March 2012 / Published online: 27 April 2012

Abstract The effect of the dispersion of zinc oxide (ZnO) nanoparticles in the zinc ion conducting gel polymer electrolyte is studied. Changes in the morphology/structure of the gel polymer electrolyte with the introduction of ZnO particles are distinctly observed using X-ray diffraction and scanning electron microscopy. The nanocomposites offer ionic conductivity values of $>10^{-3}$ S cm^{-1} with good thermal and electrochemical stabilities. The variation of ionic conductivity with temperature follows the Vogel–Tamman–Fulcher behavior. AC impedance spectroscopy, cyclic voltammetry, and transport number measurements have confirmed Zn^{2+} ion conduction in the gel nanocomposites. An electrochemical stability window from −2.25 to 2.25 V was obtained from voltammetric studies of nanocomposite films. The cationic (i.e., Zn^{2+} ion) transport number (t_+) has been found to be significantly enhanced up to a maximum of 0.55 for the dispersion of 10 wt.% ZnO nanoparticles, indicating substantial enhancement in Zn^{2+} ion conductivity. The gel polymer electrolyte nanocomposite films with enhanced Zn^{2+} ion conductivity are useful as separators and electrolytes in Zn rechargeable batteries and other electrochemical applications.

Keywords Gel polymer electrolyte · Ionic conductivity · Zinc ion transport · ZnO · Nanocomposite

Introduction

Ion conducting polymers are the materials of current interest as electrolytes/separators to replace their liquid counterparts in various solid-state ionic devices including rechargeable batteries, supercapacitors, fuel cells, etc. Solvent-free polymer–salt complexes, comprising polar polymers like poly (ethylene oxide), etc., complexed with alkali metal salts have the ability to overcome various problems commonly associated with conventional liquid electrolyte-based devices like leakage, bulky design, electrode corrosion at the interfaces, etc., and exhibit better interfacial stability [1–3]. However, their low room temperature ionic conductivity (~10^{-8}–10^{-5} S cm^{-1}) hinders their applicability in different electrochemical applications. Gel polymer electrolytes (GPEs) are recently introduced as another class of polymer-based electrolytes with improved ionic conductivity (10^{-3}–10^{-2} S cm^{-1}, comparable to liquid electrolytes) prepared by the entrapment of liquid electrolytes in different polymer hosts, e.g., poly (vinylidine fluoride-*co*-hexafluoropropylene) (PVdF-HFP), poly(methyl methacrylate) (PMMA), etc. [3–7].

As a large volume of liquid electrolyte is carried by GPEs, most of them are not dimensionally stable and the problem of leakage persists, which limit their technological applications as electrolytes. Amongst various attempts to improve their performance characteristics, the dispersion of nano-sized ceramic fillers like SiO_2, Al_2O_3, etc., to prepare nanocomposites of GPEs is an important approach which enhances their mechanical, thermal, and electrochemical characteristics. The structural modifications and changes in transport mechanism are the consequences of ion–filler and ion–polymer–filler interactions which can be greatly influenced by the size and properties of the filler particles [8–14]. Recently, Adebahr et al. [11] have shown enhancement in the diffusion of cations with the addition of TiO_2 nanoparticles in gel polymer electrolytes, while the diffusion of the solvents remains constant. The formation of micropores and reduction in crystallinity are observed when the PVdF-HFP/$LiClO_4$ matrix is dispersed with silica aerogel [12]. Li/$LiFePO_4$ solid battery composed of composite polymer electrolyte filled with mesoporous silica has been found to exhibit better cycling

Sellam · S. A. Hashmi (✉)
Department of Physics and Astrophysics, University of Delhi, Delhi 110007, India
e-mail: sahashmi@physics.du.ac.in

efficiency and capacity than the one filled with nano-sized particles [13]. Recently, our group has observed an increase in ionic conductivity by an order of magnitude in magnesium ion conducting composite gel electrolyte containing MgO and SiO_2 nanoparticles [9, 14]. It is suggested that creation of new pathways for cations in the space charge region is responsible for the improvement in cationic transport [8, 15].

To date, the rechargeable lithium battery systems are the most promising choices in view of their specific capacity and cyclic stability [16, 17]. The supremacy of lithium as anode is due to its light equivalent weight (6.941 $g eq^{-1}$), large theoretical charge capacity (3,863 Ah kg^{-1}), and higher electrode potential (−3.05 V with respect to standard hydrogen electrode) [17]. Nevertheless, these batteries are expensive and suffer from safety limitations [16–18]. Some alternatives have recently been introduced in the form of magnesium, sodium, and zinc batteries [9, 10, 14, 19–30], though they are not widely reported. Particularly, zinc metal has received attention as an anode material in zinc rechargeable batteries because of its favorable features like low cost, low toxicity, and high natural abundance. Few Zn^{2+} ion conducting polymer electrolyte systems are reported for their application in zinc batteries [29–32].

In the present paper, novel nanocomposites of zinc ion conducting gel polymer electrolytes have been reported. These comprised 1.0 M solution of zinc triflate [$Zn(Tf)_2$] in ethylene carbonate (EC)–propylene carbonate (PC) immobilized in PVdF-HFP dispersed with zinc oxide (ZnO) nanoparticles. ZnO, used as filler in the present studies, is an inorganic semiconducting material which serves as an additive in a number of materials, e.g., glass, rubber, food products, cement, paint, battery electrodes, etc. [33–36]. There are reports on ion conducting, solvent-free polymer electrolytes in which the semiconducting oxides or sulfides are dispersed to make the mixed (ion+electron) conductors [37, 38]. Such mixed conduction is not expected in the composites of gel polymer electrolytes in which the proportion of the liquid electrolyte component is large and the ionic conduction is predominantly liquid-like. Nanocomposite films have been characterized using various physical techniques such as X-ray diffraction (XRD), scanning electron microscopy (SEM), Raman spectroscopy, thermal analysis, cyclic voltammetry, impedance analysis, ionic conductivity, and transport number measurements.

Experimental

Preparation of gel nanocomposites

The copolymer PVdF-HFP (average molecular weight, ~400,000), EC, PC, zinc trifluromethanesulfonate [(zinc triflate or $Zn(Tf)_2$)], and the nano-sized ZnO powder (average particle size, <100 nm) were procured from Sigma-Aldrich and used without further purification. The salt $Zn(Tf)_2$ and ZnO nanoparticles were dried in vacuum at ~100 °C prior to use. The gel nanocomposite films were prepared using the "solution-cast" method. In this process, the liquid electrolyte was first prepared by preparing 1 M solution of $Zn(Tf)_2$ salt in a mixture of EC and PC (1:1, *v*/*v*). In general, the 1-M salt concentration in the EC/PC solution is sufficient to achieve the highest ionic conductivity at room temperature. Furthermore, the optimized ratio of EC/PC, reported by several workers, lies in the middle range, around 1:1 (*v*/*v*). The host polymer PVdF-HFP was separately dissolved in acetone at room temperature. The appropriate amount of the polymer solution (i.e., ~15 wt.% of PVdF-HFP) was mixed in liquid electrolyte. The ZnO nanoparticles were then added in the mixtures in different weight ratios from 0 to 25 wt.% with respect to PVdF-HFP and thoroughly stirred magnetically for ~10 h. Proper dispersion of ZnO particles was ensured by ultrasonicating each mixture for ~15–20 min. Finally, the mixtures were poured into glass Petri dishes and the common solvent acetone allowed to evaporate to obtain solid-like, free-standing, and flexible nanocomposite films of thickness ~100–150 μm. The gel films were stored in argon atmosphere to avoid moisture absorption. A photograph of a typical composition of nanocomposite gel film is shown in Fig. 1.

Instrumentation

Morphological changes in the gel nanocomposite films were observed using scanning electron microscope (SEM, JEOL, JSM 5600). The SEM micrographs were taken at low vacuum after sputtering the samples with gold to prepare conductive surfaces. The X-ray diffraction patterns of the films were recorded using a Phillips X-ray diffractometer with CuKα

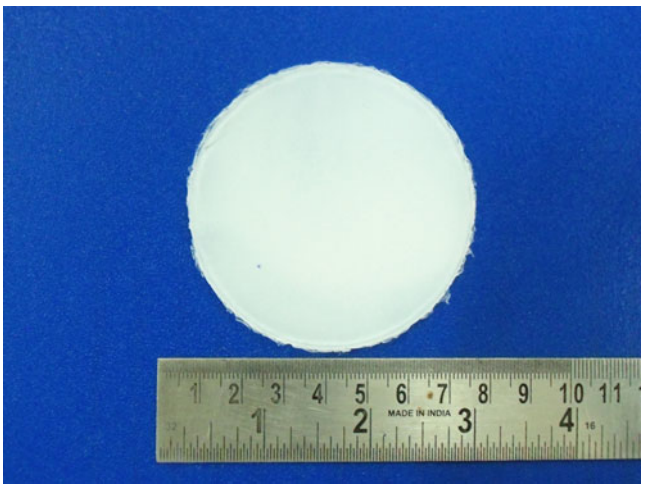

Fig. 1 Typical photograph of gel polymer electrolyte nanocomposite film EC–PC–$Zn(Tf)_2$+PVdF-HFP dispersed with 10 wt.% ZnO nanoparticles

radiation (λ=1.54 Å) in the Bragg angle (2θ) range from 5° to 70°.

Raman spectroscopic studies were performed using a Renishaw Invia Raman Microscope in a right-angled scattering geometry using the Ar ion laser. Low laser power (50 mW) was used to avoid heating of the polymer electrolyte films. The signal was detected by a CCD system. The spectral resolution was kept at 3 cm^{-1}. The samples were kept in air during measurement.

Thermal analysis of gel nanocomposite films was performed using thermogravimetric analysis (TGA) and differential scanning calorimetry (DSC). TGA was carried out from room temperature to 550 °C under a dynamic dry nitrogen atmosphere at a heating rate of 10 °C min^{-1} using a Perkin Elmer TGA system (TGA-7). DSC was performed from −90 °C to 150 °C at a heating rate of 10 °C min^{-1} in a static nitrogen atmosphere with the help of a DSC system from TA Instruments (model Q100).

Ionic conductivity measurements were performed by means of AC impedance spectroscopy with the help of a LCR Hi-Tester (model 3522-50, Hioki, Japan) over the frequency range from 1 Hz to 100 kHz at a signal level of 10 mV. The temperature dependence of conductivity was carried out over the temperature range from 30 to 85 °C. The total ionic transport number of the gel nanocomposite film was evaluated using polarization technique [39]. To employ this method, stainless steel (SS) strips were used as blocking electrodes and the cell SS|nanocomposite film|SS was polarized by applying a voltage of 1.0 V. The total (ionic+electronic) current and residual (electronic) current after a certain interval of polarization were recorded. The cationic (Zn^{2+}) transport number (t_+) of nanocomposite films was evaluated using the combination of AC impedance spectroscopy and DC polarization studies on Zn|nanocomposite gel film|Zn cells using the method of Evans et al. [40]. In accordance with this method, a small dc voltage (ΔV) was applied to polarize the cells and current was monitored as a function of time. The cells were also subjected to AC impedance measurements prior to and after the polarization to get initial and final cell resistances. The t_+ values were evaluated using the relation:

$$t_+ = \frac{I_s(\Delta V - R_0 I_0)}{I_0(\Delta V - R_s I_s)} \quad (1)$$

where I_0 and I_s are the initial and final currents and R_0 and R_s are the cell resistances before and after polarization, respectively. To evaluate the "electrochemical potential window" of the gel polymer electrolyte nanocomposites and to confirm their ability to conduct the zinc ions, cyclic voltammetric studies were performed using an electrochemical analyzer (model 608C, CH Instruments, USA).

Results and discussion

Structural and thermal studies

Comparative morphological/structural changes in the gel polymer electrolytes due to the dispersion of ZnO nanoparticles have been monitored using SEM and XRD techniques. The SEM micrographs of nanocomposite gel films containing different amounts of ZnO particles are shown in Fig. 2. The dark regions, observed in the SEM picture for undispersed gel polymer electrolyte (Fig. 2a, b), indicate the micron-sized porosity in which the liquid electrolyte can retain. On the dispersion of 10 wt.% of ZnO filler, some nano-sized white spots are distributed (Fig. 2c). These indicate the presence of nano-sized ZnO particles in the gel network as a separate phase. Furthermore, the texture and morphology of the gel polymer system has also been modified, showing smaller crystallites and pores. The changes indicate the slight interaction of the ZnO nanoparticles with the gel polymer system. A further change in the gel electrolyte texture has been observed when a larger amount (~25 wt.%) of ZnO filler is dispersed. The texture of polymer network changes so drastically that the polymer fully covers the ZnO filler particles; hence, ZnO particles appear to be disappeared in the SEM picture (Fig. 2d).

The X-ray diffraction patterns were recorded for pure PVdF-HFP and nanocomposite films dispersed with different amounts of ZnO nanoparticles along with the pure ZnO nanopowder, as shown in Fig. 3. The XRD pattern of the PVdF-HFP film shows the characteristics of a semi-crystalline microstructure with predominant peaks at 14°, 17°, 18°, 19.7°, and 38°. When the EC–PC–$Zn(Tf)_2$ solution is immobilized in PVdF-HFP, these characteristic crystalline peaks of the polymer disappear. A substantially broader hump between 10° and 30° is observed, which indicates the substantial amorphous nature of the gel polymer electrolyte. Some characteristic peaks of ZnO nanoparticles are distinctly observed at 31°, 34°, 36°, 47°, 56°, 62°, and 67° in nanocomposite gels when ZnO filler particles are dispersed (c–e in Fig. 3). This indicates that the ZnO filler particles are present in the gel system as a separate phase. The ZnO particles have also been observed as a separate phase in SEM pictures, as described earlier.

To investigate the effect of ZnO dispersion and possible conformational changes of PVdF-HFP due to liquid electrolyte entrapment, comparative Raman spectroscopic studies have been carried out for pure PVdF-HFP, gel polymer electrolyte, and its nanocomposite with different amounts of ZnO dispersion, as shown in Fig. 4. The following changes in the spectral response have been observed:

1. The prominent Raman peaks at 806 cm^{-1} (assigned to CH_2 rocking) and 884 cm^{-1} (assigned to CC(ν_s) and CCC (δ) modes) of the α-phase of the host polymer

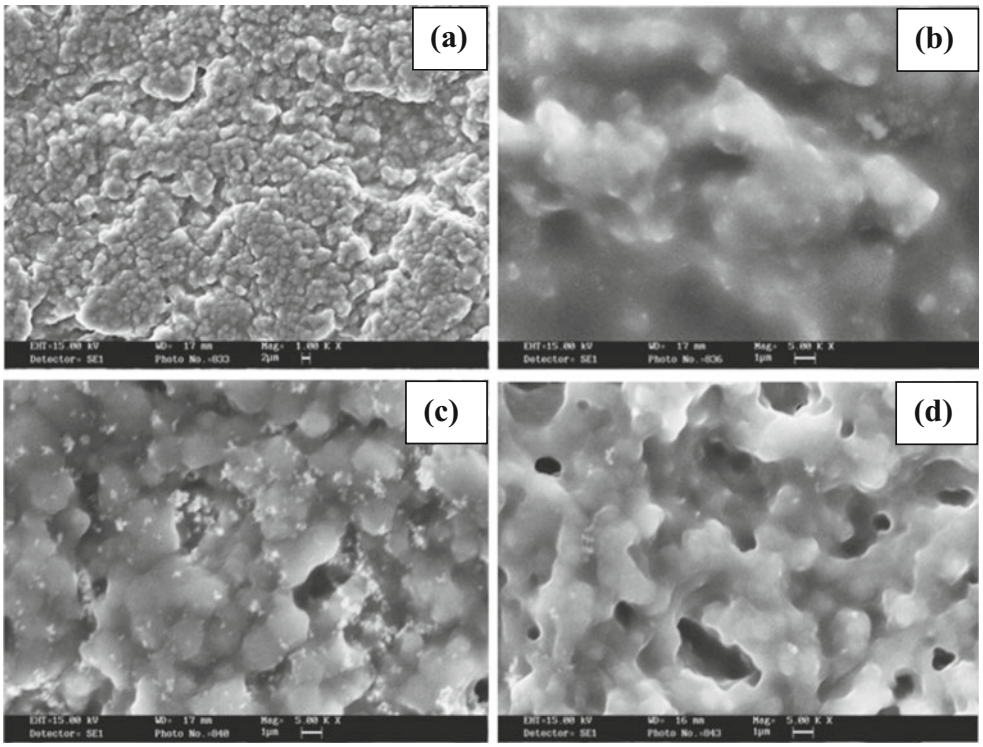

Fig. 2 SEM micrographs of EC–PC–$Zn(Tf)_2$+PVdF-HFP gel polymer electrolyte (magnification, ×1,000) (**a**); gel electrolyte with magnification ×5,000 (**b**); and its nanocomposites dispersed with ZnO particles of 10 wt.% (magnification, ×5,000) (**c**) and 25 wt.% (magnification, ×5,000) (**d**)

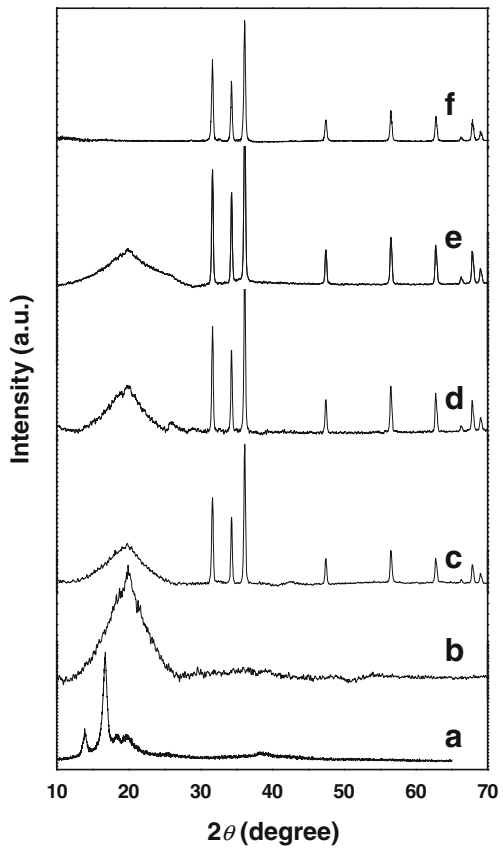

Fig. 3 XRD patterns for PVdF-HFP film (pure) (*a*), gel polymer electrolyte (*b*), and its nanocomposites dispersed with ZnO powder of 10 wt.% (*c*), 15 wt.% (*d*), and 25 wt.% (*e*) and ZnO (pure) nanopowder (*f*)

PVdF-HFP disappeared due to the entrapment of EC–PC–$Zn(Tf)_2$ liquid electrolyte, forming a gel electrolyte. Few more PVdF-HFP bands at 419, 544, and 619 cm^{-1}, attributed to the rocking and the deformation modes of CH_2 and CF_2, disappeared due to the immobilization of liquid electrolyte. The disappearance of these peaks shows a major conformational change in PVdF-HFP.

2. On dispersion of ZnO nanoparticles, significant changes in the spectral features in terms of the appearance of new prominent peaks and the disappearance of existing

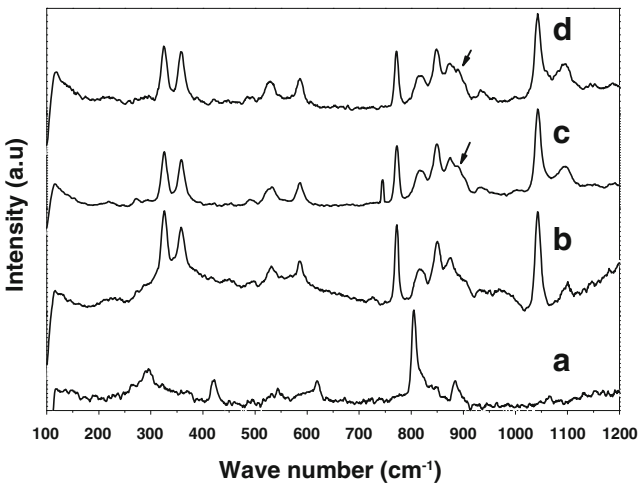

Fig. 4 Raman spectra of pure PVdF-HFP film (*a*), EC–PC–$Zn(Tf)_2$+PVdF-HFP gel polymer electrolyte (*b*), and its nanocomposites dispersed with ZnO particles of 10 wt.% (*c*) and 25 wt.% (*d*)

peaks are not observed. This shows that the ZnO nanoparticles are present in the gelled polymer matrix as a separate phase. On close inspection, however, two following changes have been obtained: (a) a shoulder appears at ~891 cm^{-1} (marked as an arrow) in the spectra of nanocomposites (c and d in Fig. 4). This is attributed to the formation of the γ-phase of the host polymer PVdF-HFP in the gel electrolyte due to the dispersion of ZnO nanoparticles [41]. The γ-phase conformation corresponds to that phase when the fluorine and the hydrogen atoms are so arranged that it possesses a permanent dipole moment [41, 42]. This change leads to the separation of hydrophilic and hydrophobic sites, which can affect the morphology of the gel polymer electrolyte membrane. (b) Raman peaks in the region 1,000–1,150 cm^{-1} corresponding to symmetric SO_3 stretching of the triflate anion are affected due to the dispersion of ZnO nanoparticles, as shown in the expanded representation of the spectra (Fig. 5). Particularly, the predominant peak at 1,042 cm^{-1}, which corresponds to the free triflate anion [43], becomes more asymmetric, and a new peak at 1,062 cm^{-1} distinctly arises due to the addition of ZnO nanoparticles. This new band at a higher wavenumber is assigned to an ion pair [43]. Furthermore, the relative intensity of the broad band at 1,095–1,097 cm^{-1} (assigned to a higher aggregate) grows with increasing contents of ZnO particles.

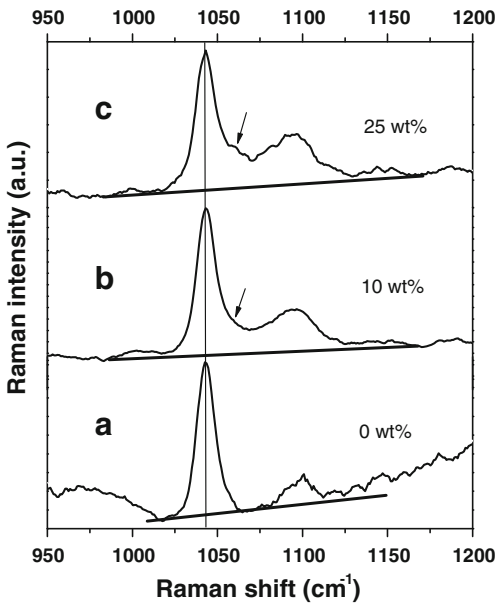

Fig. 5 Expanded representation of the Raman spectra of EC–PC–Zn $(Tf)_2$+PVdF-HFP gel polymer electrolyte (*a*) and its nanocomposites dispersed with ZnO particles of 10 wt.% (*b*) and 25 wt.% (*c*) in the 950- to 1,200-cm^{-1} spectral range

The DSC thermograms of the gel polymer electrolyte and nanocomposite gel films are shown in Fig. 6. For pure PVdF-HFP film, an endothermic peak at 140 °C is observed (a in Fig. 6), which corresponds to the melting of the polymer PVdF-HFP film [27]. Blending with a liquid electrolyte EC–PC–$Zn(Tf)_2$ lowers the melting point drastically to ~70 °C. The melting peaks become more asymmetric and broad, and this is attributed to the presence of liquid components that cause an increase in the amorphous proportion in the overall material. This melting peak shifts slightly toward a higher temperature (75–82 °C) due to the dispersion of the ZnO nanoparticles. It has also been noticed that the step changes, owing to the glass transition temperature (T_g), have also not been observed in the above temperature range. This indicates the possible shift in T_g values toward a lower temperature (i.e., less than −90 °C). The irregular patterns of the DSC curves, observed after ~110 °C, are due to the fast evaporation of volatile EC–PC components. Furthermore, no endothermic peak is found and the electrolyte films remain stable in the same gel phase over a substantially wide temperature range from −90 to 60 °C, which is advantageous for their potential applications in electrochemical devices.

The TGA curves of the gel polymer electrolyte and nanocomposite gel films with 10 and 25 wt.% of ZnO filler are shown in Fig. 7. A weight loss of ~5 wt.% has been noted for both the undispersed and dispersed gel electrolyte systems. This marginal weight loss is possibly due to the loss of surface-adsorbed moisture. A substantial weight loss has been observed subsequently due to the evaporation of PC and EC. A marginally better retentivity of PC and EC has

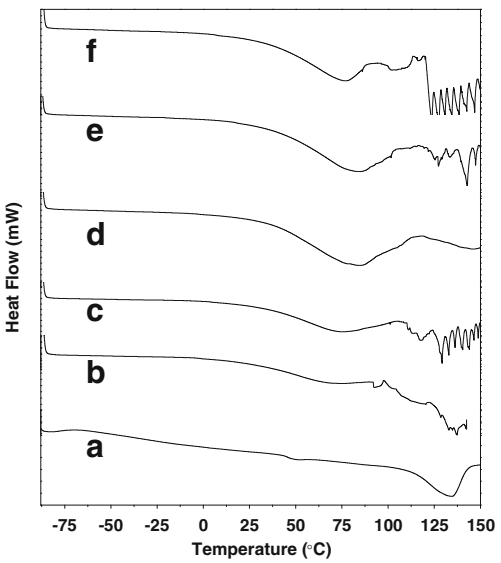

Fig. 6 DSC thermograms of the gel polymer electrolyte nanocomposites with ZnO powder of pure PVdF-HFP film (*a*), 0 wt.% (*b*), 3 wt.% (*c*), 10 wt.% (*d*), 20 wt.% (*e*), and 25 wt.% (*f*)

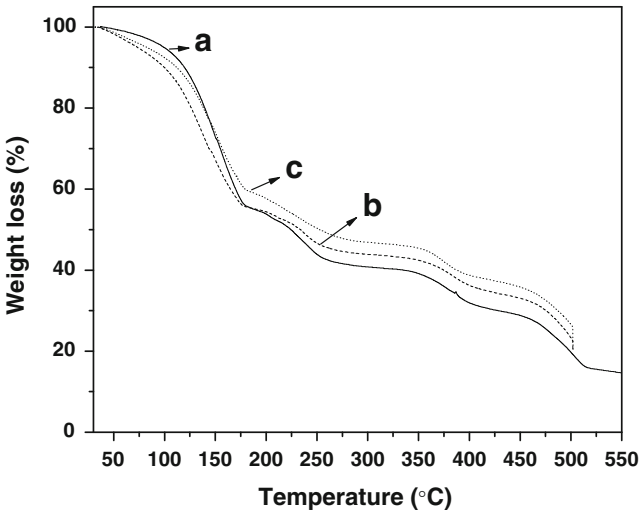

Fig. 7 TGA curves of the gel nanocomposites with ZnO powder of 0 wt.% (*solid line*) (*a*), 10 wt.% (*dash line*) (*b*), and 25 wt.% (*dotted line*) (*c*)

been noted for higher contents of ZnO nanoparticles in the gel polymer electrolyte (c in Fig. 7).

Ionic conductivity

The room temperature ionic conductivity values of the PVdF-HFP/EC–PC/$Zn(Tf)_2$ gel electrolyte films with respect to the content of dispersed ZnO nanoparticles are listed in Table 1. The ionic conductivity value of the undispersed gel polymer electrolyte is found to be ~6.7×10^{-3} S cm^{-1} at room temperature (~25 °C). The order of the conductivity has not been affected due to the dispersion of the ZnO nanoparticles. Although the ZnO nanoparticles are present in the gel system as a separate phase, as observed from SEM and XRD, it may be noted that the mechanical strength of the gel electrolyte films has been improved substantially. This indicates some interactions of the ZnO particles with the components of the gel electrolyte at the microscopic level, which has been confirmed from Raman studies discussed earlier. Furthermore, there are indications of ion pairing and aggregate formation of zinc salt due to ZnO dispersion (as observed from Raman studies). Almost no substantial loss in ionic conductivity is observed up to the 25 wt.% dispersion of ZnO nanoparticles. This is possible as Zn^{2+} ion mobility enhances due to the effect of space charge region formation in the gel system in the presence of ZnO nanoparticles, discussed in a later section.

Table 1 Room temperature ionic conductivity (σ) of EC–PC–$Zn(Tf)_2$+PVdF-HFP gel polymer electrolyte nanocomposites with respect to ZnO content

ZnO (wt.%)	σ (S cm^{-1})
0	6.7×10^{-3}
3	4.1×10^{-3}
5	6.7×10^{-3}
10	4.9×10^{-3}
12.5	5.3×10^{-3}
15	4.6×10^{-3}
20	3.1×10^{-3}
25	5.1×10^{-3}

The temperature dependence of the ionic conductivity of nanocomposite films is shown in Fig. 8. The σ vs. $1/T$ plots show the curved nature of variations which are described by the Vogel–Tamman–Fulcher (VTF) equation, given as:

$$\sigma = AT^{-\frac{1}{2}}\exp\left(\frac{-B}{T-T_0}\right) \quad (2)$$

where parameter B is associated with the rate at which viscosity changes with temperature; A is a pre-exponential factor, i.e., the conductivity at infinitely high temperature; and T_0 is the equilibrium glass transition temperature close to the actual glass transition temperature, T_g. The fitting parameters A, B, and T_0 have been estimated for all the compositions using a curve fitting method and listed in Table 2. It is observed that the typical composition of nanocomposite gel film (with ~10 wt.% ZnO particles) offers ionic conductivities of 3.7×10^{-3} S cm^{-1} at 30 °C and 1.4×10^{-2} S cm^{-1} at 85 °C, exhibiting promise for potential application as electrolyte in zinc batteries and other electrochemical applications over a wider temperature range.

CV, impedance, and transport number studies

The electrochemical potential window (ESW), another important parameter to measure the operating voltage of the

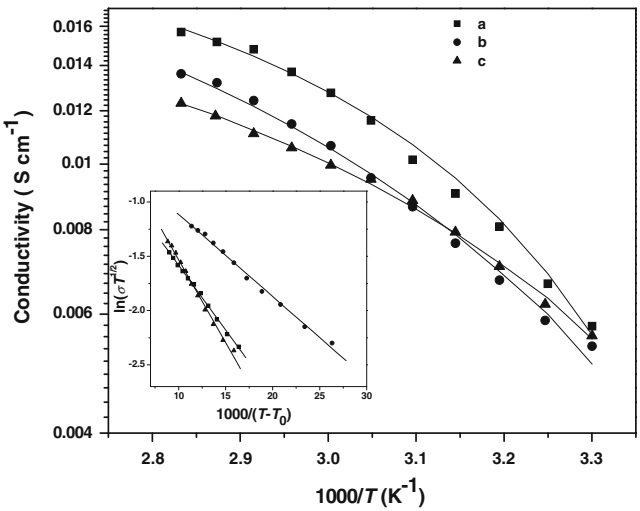

Fig. 8 σ vs. $1/T$ curves for the gel nanocomposites with ZnO powder of 0 wt.% (*a*), 15 wt.% (*b*), and 25 wt.% (*c*) (the *solid line* represents VTF fit superimposed on experimental data). The corresponding ln ($\sigma T^{1/2}$) vs. $1/(T-T_0)$ plots are shown in the *inset*

Table 2 VTF fitting parameters for gel polymer electrolyte nanocomposites

ZnO (wt. %)	A (S cm^{-1} K$^{1/2}$)	B (K)	T_0 (K)
0	0.7	75	265
5	1.155	133	253
10	0.743	108	259
12.5	0.54	65	263
15	0.99	152	240
20	0.422	82	266
25	0.675	119	242

gel nanocomposite, has been estimated using voltammetric studies on a typical cell SS|Nanocomposite with 10 wt.% ZnO|SS. As seen from the voltammogramm (Fig. 9, inset), the ESW has been found to range from −2.25 to 2.25 V (i.e., the potential window of ~4.5 V). This value of operating voltage range (i.e., ESW) is high enough to apply the Zn^{2+} ion conducting gel nanocomposite film as a solid-state-type electrolyte/separator in Zn batteries and other energy storage devices.

The comparative cyclic voltammetric studies have been performed on two cells: SS|Nanocomposite gel|SS (cell 1) and Zn|Nanocomposite gel|Zn (cell 2); the plots are shown in Fig. 9 for a typical composition of gel nanocomposite with 10 wt.% ZnO filler at the scan rate of 5 mV s^{-1}. The cathodic and anodic peaks are distinctly obtained for cell 2 with Zn electrodes, whereas such features are not observed for cell 1 with SS electrodes in the same voltage range (Fig. 9). These observations suggest an almost reversible cathodic deposition and anodic oxidation of zinc at the Zn/gel electrolyte interfaces as per the following reversible reaction:

$$Zn^{2+} + 2e^- \rightleftarrows Zn^0 \quad (3)$$

This indicates the Zn^{2+} ion conduction in the gel polymer electrolyte nanocomposite. It is observed that the anodic and cathodic peaks are separated by a few volts. Such behavior has also been obtained in other systems, e.g., Li|PEO–$LiBF_4$|Li [44], Mg|gel nanocomposites|Mg [9, 10, 14], etc., which is due to the experiments being performed on the cells with two-electrode geometry without using reference electrodes.

AC impedance spectroscopic studies on cells 1 and 2 further confirm the Zn^{2+} ion conduction in gel nanocomposite films. The comparative impedance plots are shown in Fig. 10. For cell 1, a steep rise in the impedance plot has been observed, which shows the blocking nature of SS electrodes. However, a well-defined semicircular plot has been observed for cell 2 with zinc electrodes. This shows the reversibility of the Zn/Zn^{2+} couple at the interface, which further indicates zinc ion conduction in the gel electrolyte nanocomposites.

The total ionic transport number (t_{ion}) has been evaluated using the polarization method, as described earlier. The value of t_{ion} for all the nanocomposite gel films is observed to be ~0.99 (Table 3), which indicates that the charge conduction is predominantly ionic. In the present system of gel polymer electrolytes, the Zn^{2+} cations and $CF_3SO_3^-$ anions (which are well dissociated in the aprotic medium of EC and PC) are the possible mobile ionic species. The

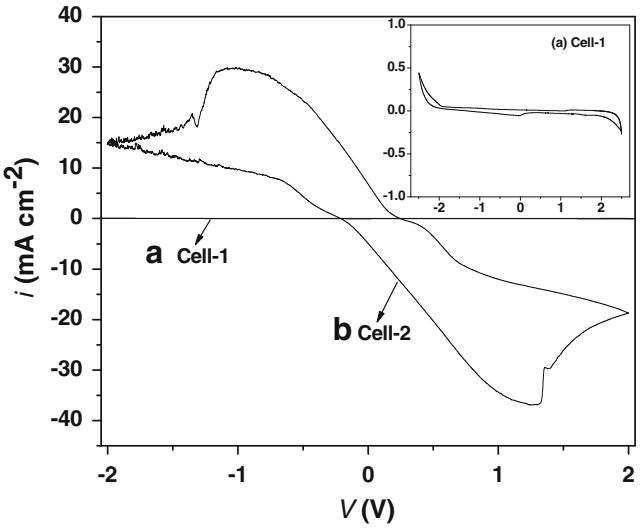

Fig. 9 Comparative cyclic voltammograms of cells—*a* SS|gel nanocomposite |SS (*Cell-1*); *b* Zn|gel nanocomposite|Zn (*Cell-2*)—recorded at room temperature at a scan rate of 5 mV s^{-1}. The cyclic voltammogram of cell SS|gel nanocomposite |SS (*Cell-1*) is shown in the *inset*. Typical gel electrolyte was EC–PC–$Zn(Tf)_2$+PVdF-HFP gel electrolyte with 10 wt.% ZnO powder

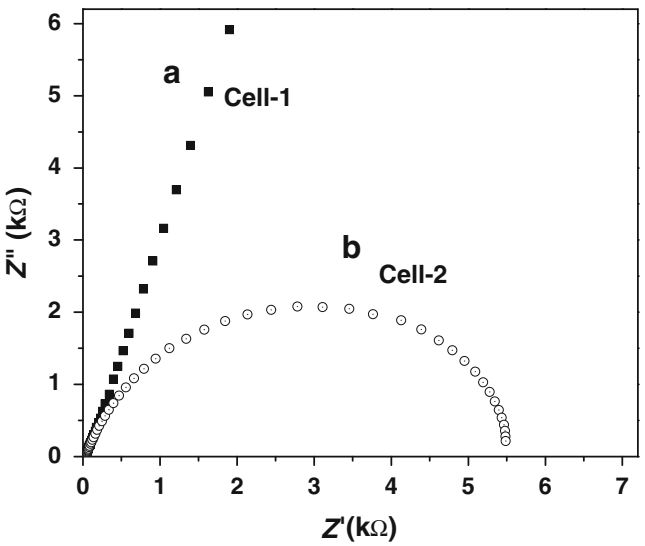

Fig. 10 AC impedance plots for *Cell-1*: SS|gel nanocomposite|SS (*a*) and *Cell-2*: Zn|gel nanocomposite|Zn (*b*) recorded at room temperature for a typical gel composition of EC–PC–$Zn(Tf)_2$+PVdF-HFP gel electrolyte with 10 wt.% ZnO powder

Table 3 Total ionic transport number (t_{ion}) and Zn^{2+} ion transport number (t_+) of gel polymer electrolytes containing different amounts of ZnO nanoparticles

ZnO (wt.%)	t_+	t_{ion}
0	0.35±0.02	~0.99
3	0.36±0.02	~0.99
5	0.55±0.02	~0.99
10	0.55±0.02	~0.99
15	0.51±0.02	~0.99
20	0.46±0.02	~0.99
25	0.47±0.02	~0.99

cationic contribution to t_{ion}, i.e., Zn^{2+} ion transport number (t_+), has been evaluated at room temperature using the method of Evans et al., as described in the previous section. The polarization curve for a typical cell, Zn|nanocomposite gel|Zn (cell 2) and the corresponding AC impedance curves to evaluate the cell resistances R_0 and R_s (before and after polarization, respectively) are shown in Fig. 11. The higher value of residual current (I_s) indicates the reversible nature of the Zn electrodes for the gel nanocomposites and further confirms Zn^{2+} ion conduction in the electrolytes. The t_+ values for gel nanocomposites containing different amounts of ZnO nanoparticles, evaluated using Eq. 1, are listed in Table 3. The Zn^{2+} ion transport number increases substantially with an increase in the amount of ZnO nanoparticles up to a maximum value of t_+=0.55 for the 10 wt.% of ZnO dispersion. Thereafter, the t_+ value slightly decreases due to the further addition of ZnO particles to the gel polymer electrolyte.

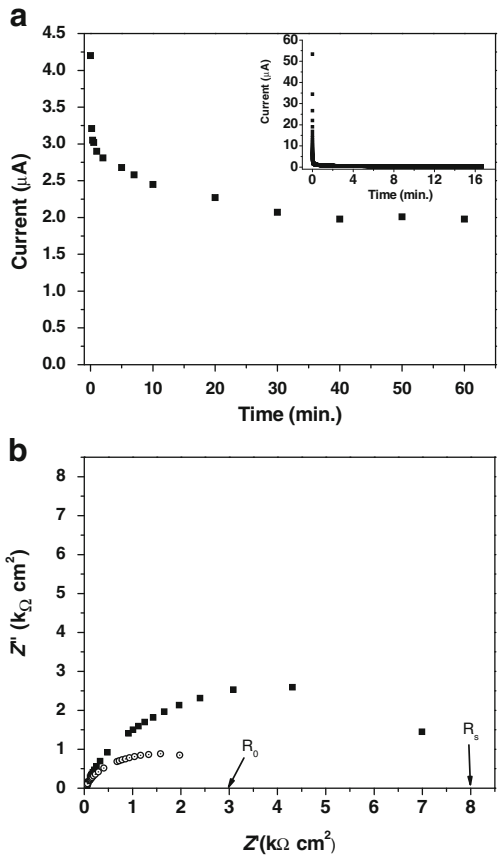

Fig. 11 **a** DC polarization curve of a typical symmetric Zn|gel nanocomposite with 5 wt.% ZnO|Zn cell at room temperature. **b** AC complex impedance plots before and after DC polarization of the cell. Applied voltage across the cell is ~34 mV. The polarization curve of cell SS|gel nanocomposite|SS at an applied voltage of 0.5 V is shown as *inset*

It may be noted that in the same range of ZnO dispersion, the overall ionic conductivity remains almost same, as discussed earlier. This indicates that the contribution of Zn^{2+} ions to the ionic conductivity increases (hence the anionic conductivity decreases) with the increasing dispersion of ZnO nanoparticles. The variation of t_+ values can be explained on the basis of space charge-mediated cationic conduction followed by blocking effect due to the dispersion of filler particles in the gel polymer electrolyte [8, 15, 45]. It is well known that the ZnO particles, used in the present system, belong to amphoteric oxides which behave as basic oxides in acidic atmosphere and shows acidic characteristics in the basic environment. The present gel electrolyte system, in which the EC–PC–$Zn(Tf)_2$ liquid electrolyte is immobilized in PVdF-HFP, offers an acidic character. The acidic nature of EC–PC–$Zn(Tf)_2$ solution was experimentally confirmed by us. The trifluoromethanesulfonate salts are generally soluble and well dissociated in dipolar aprotic solvents (e.g., PC or EC/PC mixture, etc.) [46]. The dissociated triflate anions, which are basically hard bases, have a strong tendency to form triflic acid in the presence of even a very small amount of moisture content in the electrolyte. The presence of even traces of triflic acid would form the gel system acidic. The ZnO filler particles would therefore behave as basic oxides in the acidic medium of the gel system. Under the present situation, the ZnO nanoparticles would have the tendency to attract Zn^{2+} cations from the gel electrolyte regions, and hence, there is a possibility of the following reversible reaction:

$$ZnO + Zn^{2+} \rightleftarrows ZnO : Zn^{2+} \quad (4)$$

These ZnO:Zn^{2+} species form space charge regions which induce local electric field. This local field would be responsible for enhancement in Zn^{2+} ion conduction (mobility); hence, the increase in t_+ values is obtained up to the 10 wt.% dispersion of ZnO particles. Furthermore, the ZnO nanoparticles (behaving as basic oxides) would provide additional sites for Zn^{2+} mobility within the interfacial regions formed between the gel electrolyte and filler particles. On further addition of filler particles, the decrease in t_+ values (Table 3) has been observed due to the predominantly blocking effect of filler particles in the space charge region [8, 9].

Conclusions

Non-aqueous Zn^{2+} ion conducting gel polymer electrolyte nanocomposite free-standing films have been prepared and characterized. The nanocomposite films comprise an EC–PC–$Zn(Tf)_2$ liquid electrolyte entrapped in the host polymer PVdF-HFP dispersed with nanosized ZnO filler particles. The polymer films show a semi-crystalline nature with enough porosity to retain liquid electrolyte. Conformational changes in PVdF-HFP and filler–polymer interaction have been observed due to the liquid electrolyte immobilization and dispersion of ZnO nanoparticles in the gel polymer electrolyte, as evidenced from Raman studies. The ionic conductivity of the nanocomposite gels has been found to be $>10^{-3}$ S cm^{-1} at room temperature, offering excellent thermal and electrochemical stability.

A substantial enhancement in Zn^{2+} ion transport from 0.35 to 0.55 has been achieved due to the dispersion of ZnO nanoparticles in the gel electrolytes. This leads to the enhancement in Zn^{2+} ion conductivity which is a useful achievement from the application of nanocomposites as electrolytes/separators in Zn batteries and other ionic devices.

Acknowledgments The authors acknowledge the financial support received from the Department of Science & Technology, New Delhi, and University of Delhi (under the Scheme to Strengthen R&D Doctoral Research Programme providing funds to University faculty, 11-17 Research Fund).

References

1. MacCallum JR, Vincent CA (eds) (1987) Polymer electrolyte reviews—I. Elsevier, London
2. Gray FM (1991) Solid polymer electrolytes—fundamentals and technological applications. VCH, New York
3. Agrawal RC, Pandey GP (2008) Solid polymer electrolytes: materials designing and all-solid-state battery applications: an overview. J Phys D Appl Phys 41:223001
4. Manualstephan A (2006) Review on gel polymer electrolytes for lithium batteries. Eur Polymer J 42:21–42
5. Michot T, Nishimoto A, Watanabe M (2000) Electrochemical properties of polymer gel electrolytes based on poly (vinylidene fluoride) copolymer and homopolymer. Electrochim Acta 45:1347–1360
6. Hashmi SA (2004) Supercapacitor: An emerging power source. Nat Acad Sci Lett 27:27–46
7. Sannier L, Bouchet R, Rosso M, Tarascon J-M (2006) Evaluation of GPE performances in lithium metal battery technology by means of simple polarization tests. J Power Sources 158:564–570
8. Kumar B (2004) From colloidal to composite electrolytes: properties, peculiarities, and possibilities. J Power Sources 135:215–231
9. Pandey GP, Agrawal RC, Hashmi SA (2009) Magnesium ion-conducting gel polymer electrolytes dispersed with nanosized magnesium oxide. J Power Sources 190:563–572
10. Kumar D, Hashmi SA (2010) Ion transport and ion–filler-polymer interaction in poly(methyl methacrylate)-based, sodium ion conducting, gel polymer electrolytes dispersed with silica nanoparticles. J Power Sources 195:5101–5108
11. Adebahr J, Byrne N, Forsyth M, MacFarlane DR, Jacobson P (2003) Enhancement of ion dynamics in PMMA-based gels with addition of TiO_2 nano-particles. Electrochim Acta 48:2099–2103
12. Saikia D, Chen-Yang YW, Chen YT, Li YK, Lin SI (2009) ^{7}Li NMR spectroscopy and ion conduction mechanism of composite gel polymer electrolyte: a comparative study with variation of salt and plasticizer with filler. Electrochim Acta 54:1218–1227
13. Ferrari S, Quatarone E, Mustarelli P, Magistris A, Fagnoni M, Protti S, Gerbaldi C, Spinella A (2010) Lithium ion conducting PVdF-HFP composite gel electrolytes based on N-methoxyethyl-N-methylpyrrolidinium bis(trifluoromethanesulfonyl)-imide ionic liquid. J Power Sources 195:559–566
14. Pandey GP, Agrawal RC, Hashmi SA (2011) Magnesium ion-conducting gel polymer electrolytes dispersed with fumed silica for rechargeable magnesium battery application. J Solid State Electrochem. doi:10.1007/s10008-010-1240-4
15. Maier J (1994) Defect chemistry at interfaces. Solid State Ionics 70–71:43–51
16. Tarascon JM, Armand M (2001) Issues and challenges facing rechargeable lithium batteries. Nature 414:359–367
17. Rand DAJ, Woods R, Dell RM (1998) Batteries for electric vehicles. Wiley, New York
18. Egashira M, Todo H, Yoshimoto N, Morita M (2008) Lithium ion conduction in ionic liquid-based gel polymer electrolyte. J Power Sources 178:729–735
19. Aurbach D, Lu Z, Schechter A, Gofer Y, Gizbar H, Turgeman R, Cohen Y, Moshkovich M, Levi E (2000) Prototype systems for rechargeable magnesium batteries. Nature 407:724–727
20. Noto VD, Paolo D, Vittadello M, Dall'Igna R, Boella F (2003) Potentiometric sensors with liquid polymer electrolytes based on poly ethylene glycol 400, LiCl and δ-$MgCl_2$. Electrochim Acta 48:2329–2342
21. Vittadello M, Biscazzo S, Lavina S, Fauri M, Noto VD (2002) Vibrational studies of the ion–polymer interactions in α-hydro-ω-oligo (oxyethylene) hydroxy-poly [oligo (oxyethylene) oxydimethylsililene]/δ-$MgCl_2$. Solid State Ionics 147:341–347
22. Biscazzo S, Vittadello M, Lavina S, Noto VD (2002) Synthesis and structure of electrolytic complexes based on α-hydro-ω-oligo (oxyethylene) hydroxy-poly [oligo (oxyethylene) oxydimethylsililene] and δ-$MgCl_2$. Solid State Ionics 147:377–382
23. Noto VD, Vittadello M (2002) Mechanism of ionic conductivity in poly (ethylene glycol 400)/$(MgCl_2)_x$ polymer electrolytes: studies based on electrical spectroscopy. Solid State Ionics 147:309–316
24. Noto VD, Munchow V, Vittadello M, Collet JC, Lavina S (2002) Synthesis and characterization of lithium and magnesium complexes based on $[EDTA][PEG400]_2$ and $[EDTA]_3[PEG400]_7$. Macromol Chem Phys 203:1211–1227
25. Noto VD, Vittadello M, Pace G, Biscazzo S, Lavina S (2002) Synthesis and characterization of [PEG400-*alt*-DEOS]/(δ-$MgCl_2)_{0.2597}$ complex. Macromol Chem Phys 203:1201–1210
26. Noto VD, Lavina S, Longo D, Vidali M (1998) A novel electrolytic complex based on δ-$MgCl_2$ and poly(ethylene glycol) 400. Electrochim Acta 43:1225–1237
27. Pandey GP, Hashmi SA (2009) Experimental investigations of an ionic-liquid-based, magnesium ion conducting, polymer gel electrolyte. J Power Sources 187:627–634
28. Kumar D, Hashmi SA (2010) Ionic liquid based sodium ion conducting gel polymer electrolytes. Solid State Ionics 181:416–423
29. Kumar GG, Sampath S (2003) Electrochemical characterization of poly (vinylidenefluoride)-zinc triflate gel polymer electrolyte and its application in solid-state zinc batteries. Solid State Ionics 160:289–300
30. Kumar GG, Sampath S (2005) Electrochemical and spectroscopic investigations of a gel polymer electrolyte of poly (methylmethacrylate) and zinc triflate. Solid State Ionics 176:773–780

31. Ye H, John Xu J (2007) Zinc ion conducting polymer electrolytes based on oligomeric polyether/PVDF-HFP blends. J Power Sources 165:500–508
32. Ikeda S, Mori Y, Furuhashi Y, Masuda H (1999) Multivalent cation conductive solid polymer electrolytes using photo-cross-linked polymers: II. magnesium and zinc trifluoromethanesulfonate systems. Solid State Ionics 121:329–333
33. Chang W, Choi J-W, Im J-C, Lee JK (2010) Effects of ZnO coating on electrochemical performance and thermal stability of $LiCoO_2$ as cathode material for lithium-ion batteries. J Power Sources 195:320–326
34. Wu C-G, Lu M-I, Tsai C-C, Chuang H-J (2006) PVdF-HFP/metal oxide nanocomposites: the matrices for high-conducting, low-leakage porous polymer electrolytes. J Power Sources 159:295–300
35. Fan L, Dang Z, Wei G, Nan C-W, Li M (2003) Effect of nanosized ZnO on the electrical properties of $(PEO)_{16}LiClO_4$ electrolytes. Mater Sci Eng B 99:340–343
36. Zhang Y, Sun X, Pan L, Li H, Sun Z, Sun C, Tay BK (2009) Carbon nanotube–zinc oxide electrode and gel polymer electrolyte for electrochemical supercapacitors. J Alloys and Compds 480: L17–L19
37. Chandra A, Singh PK, Chandra S (2002) Semiconductor-dispersed polymer electrolyte composites. Solid State Ionics 154–155:15–20
38. Kloster GM, Thomas JA, Brazis PW, Kannewurf CR, Shriver DF (1996) Synthesis, characterization, and transport properties of new mixed ionic−electronic conducting V_2O_5−polymer electrolyte xerogel nanocomposites. Chem Mater 8:2418–2420
39. Hashmi SA, Chandra S (1995) Experimental investigations on a sodium-ion-conducting polymer electrolyte based on poly (ethylene oxide) complexed with $NaPF_6$. Mater Sci Eng B 34:18–26
40. Evans J, Vincent CA, Bruce PG (1987) Electrochemical measurement of transference numbers in polymer electrolytes. Polymer 28:2324–2328
41. Wang K, Lee H, Cooper R, Liang H (2009) Time-resolved, stress-induced, and anisotropic phase transformation of a piezoelectric polymer. Appl Phys A 95:435–441
42. Simoes RD, Job AE, Chilanglia DL, Zucolotto V, Camargo-Filho JC, Alves N, Giacometti JA, Oliveira ON Jr, Constantino CJL (2005) Structural characterization of blends containing both PVDF and natural rubber latex. J Raman Spectrosc 36:1118–1124
43. Nunes SC, de Zea BV, Ostrovskii D, Carlos LD (2006) FT-IR and Raman spectroscopic study of di-urea cross-linked poly(oxyethylene)/siloxane ormolytes doped with Zn^{2+} ions. Vib Spectrosc 40:278–288
44. Liu Y, Lee JY, Hong L (2003) Morphology, crystallinity, and electrochemical properties of in situ formed poly(ethylene oxide)/TiO_2 nanocomposite polymer electrolytes. J Appl Polym Sci 89:2815–2822
45. Maier J (1995) Ionic conduction in space charge regions. Prog Solid State Chem 23:171–263
46. Fujinaga T, Sakamoto I (1976) Electrochemical studies of sulfonates in non-aqeous solvents. Part II. polarographic reductions of some alkaline earth and transition metal ions with sulfonate supporting electrolyte in N, N-Dimethylformamide and acetonitrile. J Electroanal Chem 73:235–246